Biomedical Optics EXPRESS

Flexible delivery of Er:YAG radiation at 2.94 μm with negative curvature silica glass fibers: a new solution for minimally invasive surgical procedures

A. Urich,[1,*] R. R. J. Maier,[1] Fei Yu,[2] J. C. Knight,[2] D. P. Hand,[1] and J. D. Shephard[1]

[1]*Applied Optics and Photonics group, School of Engineering and Physical Sciences, Heriot-Watt University, Edinburgh, EH14 4AS, UK*

[2]*Centre for Photonics and Photonic Materials, Department of Physics, University of Bath, Bath, BA2 7AY, UK*

**au36@hw.ac.uk*

Abstract: We present the delivery of high energy microsecond pulses through a *hollow-core negative-curvature fiber* at 2.94 μm. The energy densities delivered far exceed those required for biological tissue manipulation and are of the order of 2300 J/cm^2. Tissue ablation was demonstrated on hard and soft tissue in dry and aqueous conditions with no detrimental effects to the fiber or catastrophic damage to the end facets. The energy is guided in a well confined single mode allowing for a small and controllable focused spot delivered flexibly to the point of operation. Hence, a mechanically and chemically robust alternative to the existing Er:YAG delivery systems is proposed which paves the way for new routes for minimally invasive surgical laser procedures.

OCIS codes: (060.2270) Fiber characterization; (060.2430) Fibers, single-mode; (060.5295) Photonic crystal fibers; (170.1020) Ablation of tissue; (170.3890) Medical optics instrumentation.

References and links

1. C. W. Robertson and D. Williams, "Lambert absorption coefficients of water in the infrared," J. Opt. Soc. Am. **61**(10), 1316–1320 (1971).
2. S. Stübinger, B. von Rechenberg, H. F. Zeilhofer, R. Sader, and C. Landes, "Er:YAG laser osteotomy for removal of impacted teeth: clinical comparison of two techniques," Lasers Surg. Med. **39**(7), 583–588 (2007).
3. J. S. Sanghera, L. B. Shaw, and I. D. Aggarwal, "Applications of chalcogenide glass optical fibers," C. R. Chim. **5**(12), 873–883 (2002).
4. N. J. Scott, R. A. Barton, A. L. Casperson, A. Tchapyjnikov, K. Levin, D. Tran, and N. M. Fried, "Mid-IR germanium oxide fibers for contact erbium laser tissue ablation in endoscopic surgery," IEEE J. Sel. Top. Quantum Electron. **13**(6), 1709–1714 (2007).
5. N. M. Fried, Y. B. Yang, C. A. Chaney, and D. Fried, "Transmission of Q-switched erbium:YSGG (λ=2.79 μm) and erbium:YAG (λ=2.94 μm) laser radiation through germanium oxide and sapphire optical fibres at high pulse energies," Lasers Med. Sci. **19**(3), 155–160 (2004).
6. A. Hongo, M. Miyagi, Y. Kato, M. Suzumura, S. Kubota, Y. Wang, and T. Shimomura, "Fabrication of dielectric-coated silver hollow glass waveguides for the infrared by liquid-flow coating method," Proc. SPIE **2677**, 55–63 (1996).
7. J. A. Harrington, "A review of IR transmitting, hollow waveguides," Fiber Integrated Opt. **19**(3), 211–227 (2000).
8. B. F. Bowden and J. A. Harrington, "Fabrication and characterization of chalcogenide glass for hollow Bragg fibers," Appl. Opt. **48**(16), 3050–3054 (2009).
9. O. Humbach, H. Fabian, U. Grzesik, U. Haken, and W. Heitmann, "Analysis of OH absorption bands in synthetic silica," J. Non-Cryst. Solids **203**, 19–26 (1996).
10. J. D. Shephard, W. N. Macpherson, R. R. J. Maier, J. D. C. Jones, D. P. Hand, M. Mohebbi, A. K. George, P. J. Roberts, and J. C. Knight, "Single-mode mid-IR guidance in a hollow-core photonic crystal fiber," Opt. Express **13**(18), 7139–7144 (2005).

#176638 - $15.00 USD Received 20 Sep 2012; revised 14 Dec 2012; accepted 19 Dec 2012; published 21 Dec 2012

11. J. D. Shephard, J. D. C. Jones, D. P. Hand, G. Bouwmans, J. C. Knight, P. S. Russell, and B. J. Mangan, "High energy nanosecond laser pulses delivered single-mode through hollow-core PBG fibers," Opt. Express **12**(4), 717–723 (2004).
12. J. D. Shephard, P. J. Roberts, J. D. C. Jones, J. C. Knight, and D. P. Hand, "Measuring beam quality of hollow core photonic crystal fibers," J. Lightwave Technol. **24**(10), 3761–3769 (2006).
13. J. D. Shephard, F. Couny, P. S. Russell, J. D. C. Jones, J. C. Knight, and D. P. Hand, "Improved hollow-core photonic crystal fiber design for delivery of nanosecond pulses in laser micromachining applications," Appl. Opt. **44**(21), 4582–4588 (2005).
14. F. Yu, W. J. Wadsworth, and J. C. Knight, "Low loss silica hollow core fibers for 3-4 μm spectral region," Opt. Express **20**(10), 11153–11158 (2012).
15. A. Urich, T. Delmonte, R. R. J. Maier, D. P. Hand, and J. D. Shephard, "Towards implementation of hollow core fibres for surgical applications," Proc. SPIE **7894**, 78940W (2011).
16. M. C. Pierce, M. R. Dickinson, and H. Devlin, "Selective photothermal ablation of tissue with a fibre delivered Er: YAG laser," Proc. SPIE **3601**, 362–368 (1999).
17. U. Hohenleutner, S. Hohenleutner, W. Bäumler, and M. Landthaler, "Fast and effective skin ablation with an Er:YAG laser: determination of ablation rates and thermal damage zones," Lasers Surg. Med. **20**(3), 242–247 (1997).
18. T. Wesendahl, P. Janknecht, B. Ott, and M. Frenz, "Erbium: YAG laser ablation of retinal tissue under perfluorodecaline: determination of laser-tissue interaction in pig eyes," Invest. Ophthalmol. Vis. Sci. **41**(2), 505–512 (2000).
19. Y. Nishimoto, M. Otsuki, M. Yamauti, T. Eguchi, Y. Sato, R. M. Foxton, and J. Tagami, "Effect of pulse duration of Er: YAG laser on dentin ablation," Dent. Mater. J. **27**(3), 433–439 (2008).
20. J. P. Parry, T. J. Stephens, J. D. Shephard, J. D. C. Jones, and D. P. Hand, "Analysis of optical damage mechanisms in hollow-core waveguides delivering nanosecond pulses from a Q-switched Nd:YAG laser," Appl. Opt. **45**(36), 9160–9167 (2006).
21. M. Contente, F. de Lima, R. Galo, J. Pécora, L. Bachmann, R. Palma-Dibb, and M. Borsatto, "Temperature rise during Er:YAG cavity preparation of primary enamel," Lasers Med. Sci. (preprint) http://www.springerlink.com/index/Q24548Q541Q6017U.pdf.
22. J. T. Walsh, Jr. and T. F. Deutsch, "Er:YAG laser ablation of tissue: measurement of ablation rates," Lasers Surg. Med. **9**(4), 327–337 (1989).
23. N. M. Litchinitser, A. K. Abeeluck, C. Headley, and B. J. Eggleton, "Antiresonant reflecting photonic crystal optical waveguides," Opt. Lett. **27**(18), 1592–1594 (2002).
24. Z. Huang, F. Fu, Z. Zhong, L. Zhang, R. Xu, and X. Zhao, "Flexible ureteroscopy and laser lithotripsy for bilateral multiple intrarenal stones: is this a valuable choice?" Urology **80**(4), 800–804 (2012).
25. J. Raif, M. Vardi, O. Nahlieli, and I. Gannot, "An Er:YAG laser endoscopic fiber delivery system for lithotripsy of salivary stones," Lasers Surg. Med. **38**(6), 580–587 (2006).
26. D. G. Kotsifaki and A. A. Serafetinides, "Mid-infrared radiation transmission through fluoride glass multimode optical fibers," Opt. Laser Technol. **43**(8), 1448–1452 (2011).
27. D. G. Kotsifaki and A. A. Serafetinides, "Pulsed infrared radiation transmission through hollow silica waveguides," Opt. Laser Technol. **41**(4), 365–373 (2009).
28. J. Albert and G. L. Yip, "Insertion loss reduction between single-mode fibers and diffused channel waveguides," Appl. Opt. **27**(23), 4837–4843 (1988).

1. Introduction

Er:YAG lasers emitting at a wavelength of 2.94 μm are widely used in medicine. The wide application of this laser in medical procedures is due to the high absorption coefficient of water contained in biological tissue of around 12000 cm^{-1} at this wavelength [1]. This leads to the unique capability of a small penetration depth and therefore high ablation rates, with high precision and a minimal heat-affected zone. This is key to reducing collateral damage, or cell death in surrounding tissue, during surgical procedures. Additional generic advantages of laser based procedures are that no pressure is applied, reducing the pain for the patient, e.g., in dental drilling [2], and the cut geometry is not limited by the drill/scalpel geometry but is dictated by the focused spot size which generally can be significantly smaller than traditional surgical tools.

In order to harness the advantages of lasers for medical procedures the laser light should ideally be delivered via a flexible guide from the laser source to the patient, allowing complete freedom for the surgeon. Several delivery systems are already in use to deliver the necessary powers to manipulate (i.e., cut and drill) biological/human tissue. The two most common ones are articulated arms and large core multimode optical fibers. The articulated arm is a system of rigid tubes connected by movable joints with built in mirrors and an

#176638 - $15.00 USD Received 20 Sep 2012; revised 14 Dec 2012; accepted 19 Dec 2012; published 21 Dec 2012

interchangeable hand piece. The hand piece contains optics to generate a particular beam profile on the tissue to be processed. There has been continued improvement of these systems and early issues, like beam wandering when the arm was moved, have been largely overcome. However, such arms can never be completely flexible in 3D space, restricting the surgeon. Generally, the size of the hand piece prevents the use of the articulated arm in minimally invasive surgery or in combination with endoscopy, although by attaching a short fiber to the hand piece some of these space restrictions are eliminated.

The alternative to the articulated arm would be to use a robust and flexible fiber delivery system. The main drive for fiber delivery is the flexibility it gives the users and the small physical size and weight which would therefore drastically increase the usability of these surgical lasers. There are a number of solid core fibers operating at the wavelength of 2.94 μm, that have been investigated for this application, based on chalcogenides [3,4], GeO_2 [4] or sapphire [5]. All these fiber types were demonstrated to deliver high power multimode laser beams.

In solid core fibers the laser induced damage threshold (LIDT) of the fiber material imposes a limit on the power handling capabilities. In order to circumvent such issues hollow core fibers have been developed. The main types of these fibers guide by Bragg reflection, or by internal reflection at a dielectric coated metallic interface in the case of the leaky tube waveguide [6–8]. However, these types of waveguides are limited in length due to the fabrication process. Hollow core photonic crystal fibers (HC-PCF) have been shown to guide in this wavelength region with power handling capabilities suited to laser surgery [9]. Since in these waveguide designs the light is mainly guided inside the hollow core of the fiber, they typically have a higher damage threshold than solid core fibers [10–13].

In this paper the application of a new fiber design based on the principles of hollow core microstructured fibers to surgery is described. Due to the shape of the central hollow core geometry, as shown Fig. 1 [14], this fiber is referred to as a Negative Curvature Fiber (NCF). The fiber is fabricated [14] from fused silica using a conventional stack and draw technique similar to that used for HC-PCF. The material is Suprasil F300 which has a bulk attenuation of ~50 dB/m at 2.94 μm (see Fig. 2) [9]. However, as light is mainly confined to the hollow core the influence of this high absorption is significantly reduced allowing low-loss fibers to be made in this wavelength region [10,15]. Silica is a desirable material for medical applications as it has several advantages, e.g., it can withstand high temperatures, it is bio-inert, mechanically and chemically robust and it has been extensively characterized for fiber drawing which makes it easy to handle. The broadband guidance of the fiber has been

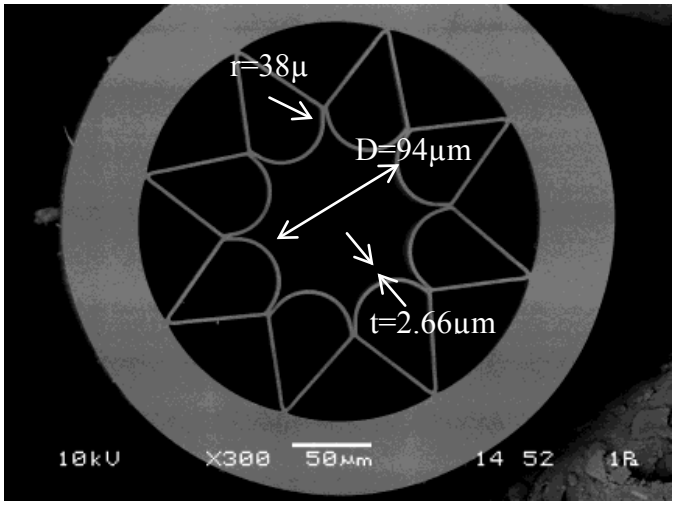

Fig. 1. SEM picture of the negative curvature fiber used in these experiments.

#176638 - $15.00 USD Received 20 Sep 2012; revised 14 Dec 2012; accepted 19 Dec 2012; published 21 Dec 2012

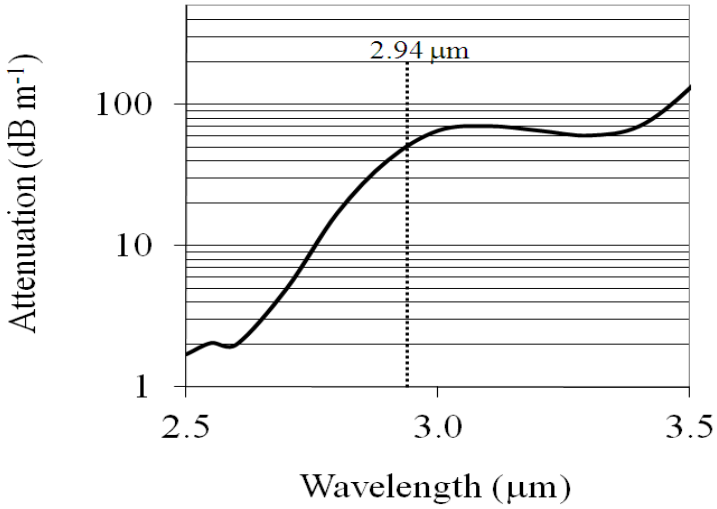

Fig. 2. Absorption spectrum of silica (Suprasil F300) in the mid IR [9].

previously described, with low attenuation ranges from 2 μm to 2.5 μm and from 2.8 μm to 3.8 μm [14]. The lowest attenuation achieved was 34 dB/km at 3.05 μm. In this paper the fiber presented in [14] was used to demonstrate the high energy laser pulse delivery of 2.94 μm radiation for use as a flexible delivery system for surgical lasers.

In order to be considered as an alternative solution for flexible delivery of Er:YAG laser light the fiber must reliably deliver pulses of sufficient energy to ablate a wide range of biological tissue. The typical thresholds required as reported in the literature are shown in Table 1. As described in this paper, the energy density transmitted through this fiber far exceeds the thresholds required for hard and soft biological tissue ablation.

Table 1. Ablation thresholds for different biological tissues

Rep rate [Hz]	Pulse length [μs]	Tissue type	Threshold [J/cm^2]	Refs.
2	250	Human dental enamel	35	[16]
7-10	250	Human skin	1.6	[17]
1.7	250	Pig retina	1	[18]
1	100-5000	Human dentine	2.69-3.66	[19,20]
5	NA	Pig skin (vitro)	3.6-5.6	[21]
2	200	Guinea pig skin	0.6-1.5	[22]

2. Laser and optics

The laser used in our experiments was an Impex High Tech ERB 15 laser. The operating wavelength is 2.937 μm and the pulse-length is 225 μs FWHM (Fig. 3a), with an M^2 of ~2.5 at a repetition rate of ~15 Hz. The spatial profile of the laser output has a donut shape (Fig. 3b); the low resolution in the image is a result of the relatively large pixel size of the IR camera used (each pixel is 50 × 50 μm). The laser light was coupled into the fiber using a lens of focal length f = 100 mm, giving a focused spot size diameter of 67 μm and focused cone angle of 70 mrad.

This optical arrangement was found to give the best coupling efficiency but due to the mismatch between the laser mode and the fiber mode field profile (which is a Gaussian-like single mode) the maximum coupling efficiency achieved was around 35%. This coupling efficiency was independent from the incident energy level. It is possible to improve the laser beam profile, i.e., achieve a smaller M^2 value by inserting an aperture in the laser cavity but this resulted in a significant loss of output power and consequently the donut mode was used

#176638 - $15.00 USD Received 20 Sep 2012; revised 14 Dec 2012; accepted 19 Dec 2012; published 21 Dec 2012

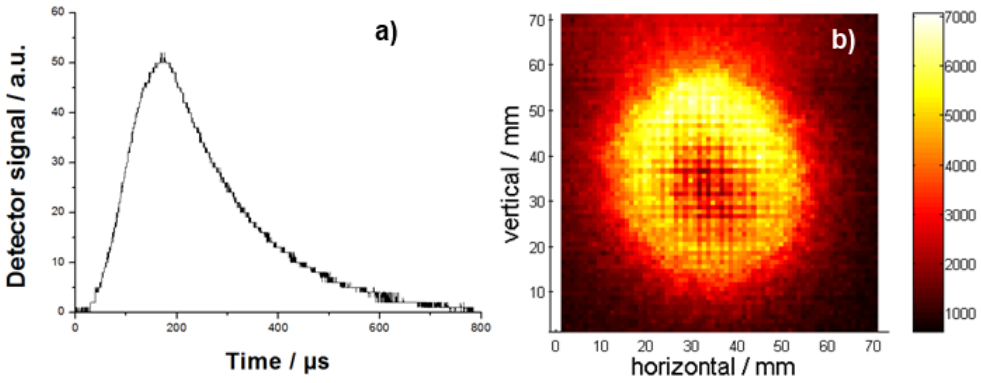

Fig. 3. (a) Temporal profile of the laser pulse (b) Spatial beam profile of the laser showing a donut shaped beam.

to excite the fiber for all experiments. It is assumed that modes that have not been coupled into the core mode couple into cladding modes. These cladding modes are gradually absorbed over a short length in the outer fused silica cladding and the protective polyimide jacket on the outside of the fiber. The absorption of fused silica at this wavelength is around 50 dB/m [9]. Since the cladding modes are leaking away over a distance, the localized energy deposition in the fused silica cladding is reduced and no measures had to be taken to cool the fiber, and importantly, no damage from the absorbed energy was observed.

3. Fiber

The guidance of this fiber can be explained by the Anti-resonant reflecting optical waveguide (ARROW) principle [23]. As described by Litchinitser et al. [23], wavelengths which are in resonance with the core wall cannot be confined in the core but leak away thought the wall, resulting in a high attenuation. However, frequencies that are anti-resonant with the wall cannot propagate within it and will be more confined inside the core. The two interfaces of wall and air can be described as a Fabry-Perot-like resonator. Anti-resonant wavelengths experience a low leakage through the wall and hence a lower attenuation as a result of destructive interference in the Fabry-Perot resonator.

Fabrication of the fiber was performed using a standard stack and draw method, as described in reference [14]. The core diameter (defined as the shortest distance inside the core) is 94 µm, and the angle of the full acceptance cone is 60 mrad (NA of 0.03).

3.1. Attenuation

To measure the attenuation of the fiber at 2.94 µm a cut back measurement was carried out, using a tunable laser as the optical source. The total attenuation in these NCF fibers is a combination of confinement and absorptive losses and bend induced losses. We therefore took great care to ensure the fiber was bent in a known and defined manner. The ends of the fiber were held straight and the fiber was bent with a diameter of 50 cm. The bent part of the fiber consisted of 5.5 full circles. The initial length of the fiber was 9.55 m and a 3 m long piece was cut back, which corresponds to two full circles. The attenuation measured for this configuration, where 5.5 m of the fiber is coiled with a diameter of 0.5 m and 0.5 m straight fiber at either end, was measured to be 0.183 dB/m ± 0.05 dB/m.

Figure 4 shows the additional losses that accrue if the fiber is bent by 180° with diameters from 50 cm down to 5 cm for 1.23 m long fiber piece. As can be seen there are no significant additional loses if the bend diameter is >30 cm, which is sufficient for many applications. The bending losses are most likely from core mode(s) coupling into cladding modes which are strongly absorbed. From the same graph it is noticeable that the attenuation for shorter wavelengths for a bend diameter of 20 cm is higher than for 10 cm. The details of this

#176638 - $15.00 USD Received 20 Sep 2012; revised 14 Dec 2012; accepted 19 Dec 2012; published 21 Dec 2012

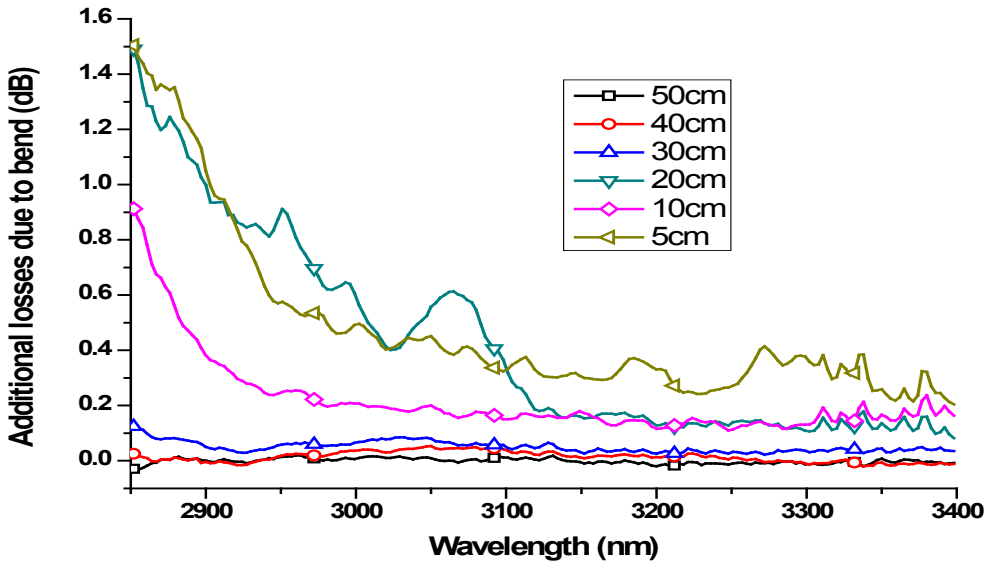

Fig. 4. Additional losses due to fiber bend in dB for a 1.23 m long fiber piece. The bend diameter is given for one 180° bend.

unexpected behavior—which is presumably due to coupling to other modes in the fiber—are yet to be investigated. Output beam mode profiles for shorter wavelengths could give an indication of the potential mode coupling at tighter bends, and it is our intention to address this in future work.

Typical bend diameters needed for endoscopy applications, such as endourology are of the order of 15 cm [24]. Such bend radii are possible with solid core sapphire fibers but for flexibility need core diameters below 600 µm which therefore imposes a damage threshold on the fiber [25]. State-of-the-art multimode solid core fiber delivery systems based on fluoride glasses can achieve a bending diameter of 20 cm with very weak dependence on the bend diameter [26] and having an attenuation of ~0.2 dB/m. Alternatively, multimode hollow core waveguides have shown a higher dependence between the bend diameter and losses. The attenuation for a hollow core waveguide with a 750 µm core has been reported as 1.9 dB/m (90° bend) and 2.9 dB/m (180° bend) when the bend diameter was 30 cm [27]. However, it is envisaged that in order to develop novel minimally invasive procedures it may be necessary have bend diameters in the order of 10's mm.

3.2. Fiber output beam profile

An investigation of the fiber output beam profile was carried out by moving a second fiber transversal to the negative curvature fiber (NCF). The "measuring" fiber used was a previously reported HC-PCF with a band gap at 2.94 µm, core diameter of 24 µm and a single mode core profile [15]. This measurement, using a smaller-core fiber for signal collection, significantly increase the fidelity of the convolution which was present in the earlier similar measurement [14] using two identical fibers. The output power of the HC-PCF was measured with a pyroelectric detector (Coherent P5-01). The position of the fiber was controlled with a LVDT (Linear Variable Differential Transformer) (Tesa Tronic TTD20). The relative output power versus the fiber position is shown in Fig. 5. The fiber was bent during this test to a bend diameter of ~50 cm.

As can be seen from the measurement, the output beam profile is single mode like and close to a Gaussian beam profile. The beam profiles are identical for straight and bent fiber configurations. From this measurement a $1/e^2$ mode field diameter of 78 µm can be calculated which is 83% of the core diameter and demonstrates good confinement in the hollow core.

#176638 - $15.00 USD Received 20 Sep 2012; revised 14 Dec 2012; accepted 19 Dec 2012; published 21 Dec 2012

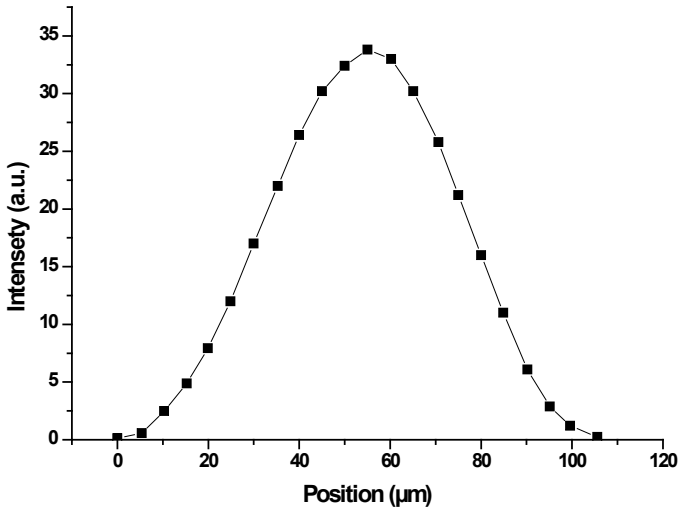

Fig. 5. Fiber output beam profile for a bent NCF measured by moving a HC- PCF transversally relative to the NCF. The NCF was bent with a diameter of ~50 cm over a length of 80 cm.

The M^2 of the fiber-delivered beam was measured (according to ISO Standard 11146 [12]) as 1.4 which is in line with the Gaussian like output beam profile shown in Fig. 5.

Modeling was done to estimate the overlap between the laser and the fiber mode in order to indicate the maximum coupling efficiency achievable. This was done by a calculation of the overlap integral, I, of the amplitudes of the laser mode, φ_{laser}, and the fiber mode, φ_{fiber}, where

$$I = \frac{\left(\iint_{-\infty}^{\infty} \varphi_{fiber}\varphi_{laser}\,dxdy\right)^2}{\left(\iint_{-\infty}^{\infty} \varphi_{fiber}{}^2\,dxdy\right)\left(\iint_{-\infty}^{\infty} \varphi_{laser}{}^2\,dxdy\right)} \quad (1)$$

as described in [28]. As only a 1D spatial prolife of the fiber output was measured for this calculation the fiber mode profile at input was assumed to be a Gaussian beam profile with the same $1/e^2$ beam diameter as the fiber (78 μm). The overlap of this assumed fiber mode and the laser beam mode as calculated from Eq. (1) is 55.8%. As can be seen from the measurement, the output beam profile is single mode like and close to a Gaussian beam profile. Based on the profile in Fig. 5 the fiber output has a 98.7% overlap with a perfect Gaussian of the same $1/e^2$ beam width.

3.3. Beam propagation

It is envisaged that the fiber could be used in contact mode or with a standoff from the tissue in practical medical procedures. Consequently an investigation of the far field propagation was carried out to assess the spatial beam profile at certain distances from the fiber end facet. To assess the spatial beam profile the beam was incident on a ceramic surface and an image was captured with a mid-infrared camera (Electrophysics PV320 L2E). The fiber used for these images had a length of 6.48 m and was curled up in a loop with a diameter of 50 cm over a length of 5.5 m. The distances between the fiber end and the reflective surface were 10, 20, 50 and 100 mm, respectively to replicate what could be conceived as practical working distances for surgery. The false color images are shown in Fig. 6. No significant change in the general beam profile can be detected other than the expected increase in beam diameter for distances from 10 mm to 100 mm.

#176638 - $15.00 USD Received 20 Sep 2012; revised 14 Dec 2012; accepted 19 Dec 2012; published 21 Dec 2012

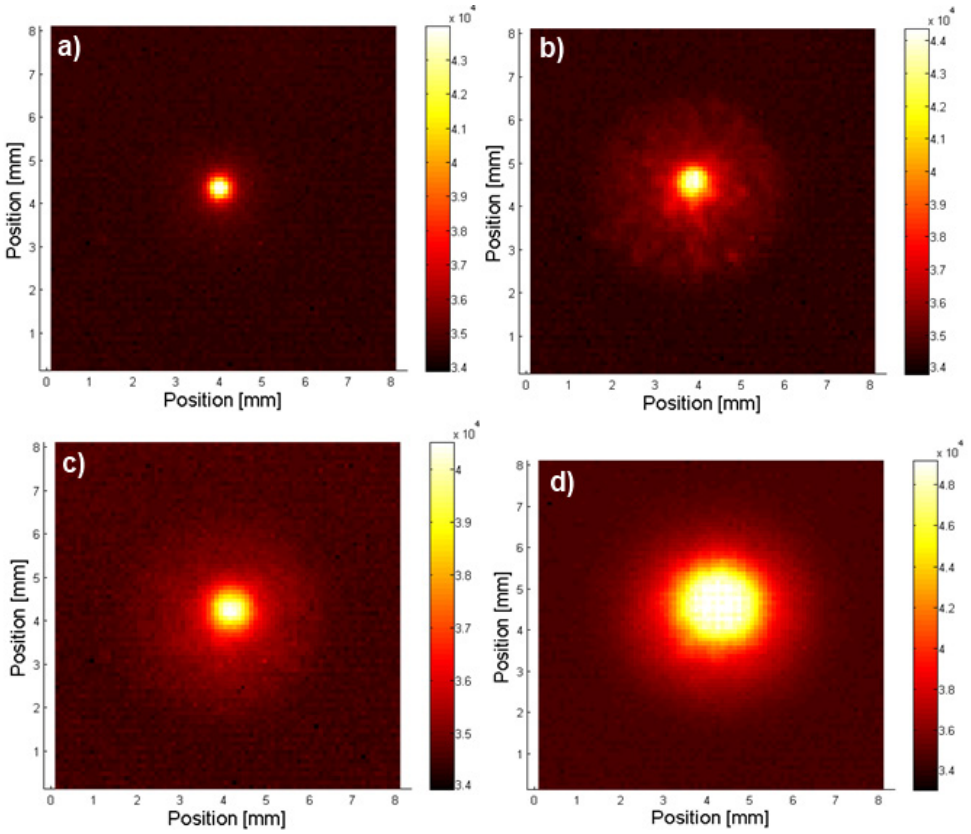

Fig. 6. Far field beam profile at different distances (a) 10, (b) 20, (c) 50, and (d) 100 mm) from the fiber end. The fiber length is 6.48 m.

3.4. High energy microsecond pulse delivery

The maximum output energy delivered through the NCF was achieved when the full power output of the laser was incident at the input of the fiber, resulting in an energy at the output of the fiber of 195 ± 1 mJ for a 33 cm length of fiber and 54 ± 4 mJ for a 9.88 m length. In both cases the fiber was bent to a diameter of 50 cm over a length of 80 cm. These pulse energies translate to energy densities of 2300 J/cm^2 for the short length and 764 J/cm^2 for the long length immediately at the end of the fiber, respectively. As shown in Table 1, human dental enamel has the highest ablation threshold of 35 J/cm^2, and it is clear that even for the longer 10 m fiber the delivered energy density exceeds it by a factor of >21. It should also be noted that the stated values for the power delivery capability of the fiber do not represent the limits of the power handling capability of the fiber as the experiment was limited by the available power from the laser source. Both the input and output facets of the fiber were undamaged during the transmission experiments. It is likely that given a laser with higher output energy and/or better beam quality, significantly higher pulse energies could be delivered.

To test the practicality of the fiber it was used free handed to ablate material. During these tests the fiber was bent down to a diameter of <10 cm. No damage to the fiber could be detected although the power output dropped as expected due to increased bend loss, however it was still sufficient enough to ablate the material (porcine bone).

4. Encapsulation of the fiber with an endtip

One practical issue in using hollow-core fibers for medical applications is the possibility of contaminating the core with debris and liquids (e.g., blood or tissue fragments) particularly if

#176638 - $15.00 USD Received 20 Sep 2012; revised 14 Dec 2012; accepted 19 Dec 2012; published 21 Dec 2012

the fiber is used in an endoscopic procedure. Therefore an encapsulation of at least one fiber end is necessary. Our approach is the sapphire endtip and a schematic is shown in Fig. 7. As a demonstrator this endtip was mounted onto the fiber using a heat shrinking tube (Fig. 8).

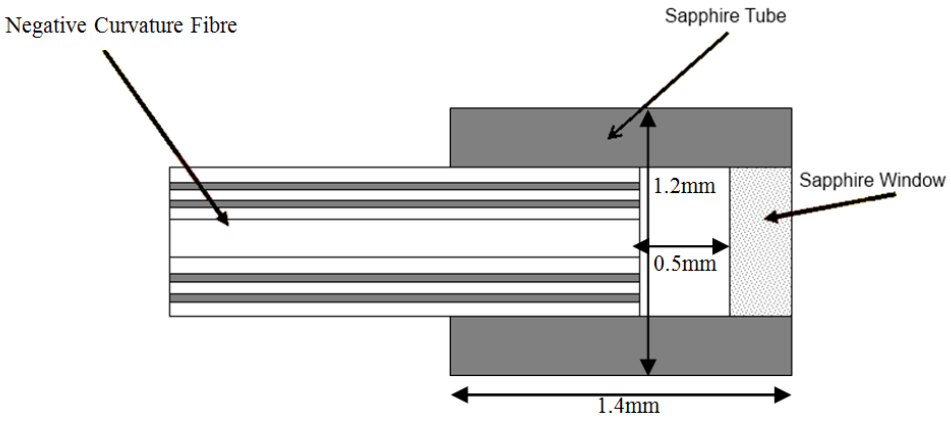

Fig. 7. schematic and dimensions of the sapphire endtip.

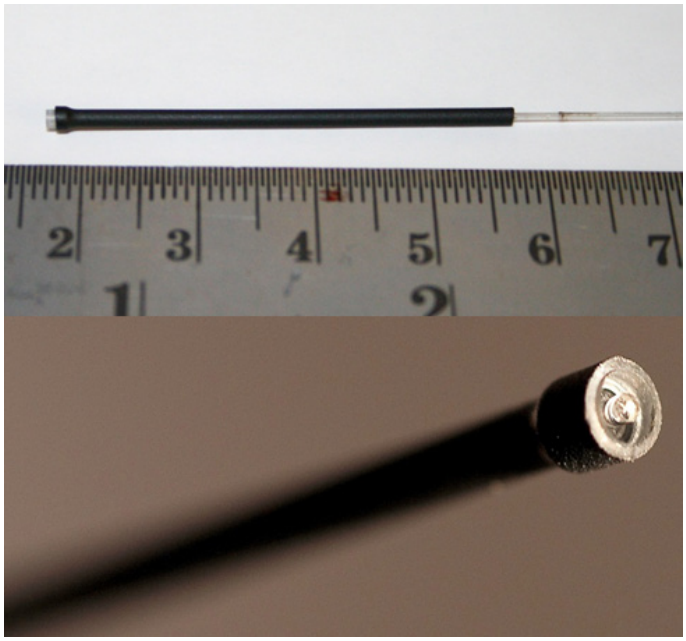

Fig. 8. Endtip mounted onto the fiber using a heat shrinking tube.

The distance between the fiber end facet and the outer surface of the sapphire window in the endtip (the contact point of laser irradiation and tissue) is 0.5 mm. In order to avoid damage to the sapphire window of the endtip the energy was restricted for these tests as it still provided sufficient energy for tissue ablation. The maximum output energy measured at this point using a 2 m long fiber piece was 30 mJ. Using this value and the divergence half angle of 36 mrad gives an energy density of >500 J/cm^2 at the contact point. Again this energy density far exceeds the ablation thresholds necessary for biological tissue yet is well within the operating capability of the device.

A cross section through the spatial beam profile directly at the end of the tip is shown in Fig. 9. Although there is some change in the beam profile compared to the previous image (Fig. 5) it is not significantly different and the beam is still single-mode-like.

#176638 - $15.00 USD Received 20 Sep 2012; revised 14 Dec 2012; accepted 19 Dec 2012; published 21 Dec 2012

This figure represents the beam profile incident on the tissue if the fiber is used in contact mode, where the endtip would be in direct contact with the tissue. The far field output beam profile at distances of 10, 20, 50 and 100 mm are also shown, again to demonstrate conditions expected for practical surgical applications, Figs. 10(b) and 10(c). Compared to the beam profile without an endtip (Fig. 6) some artifacts around the central peak position are visible

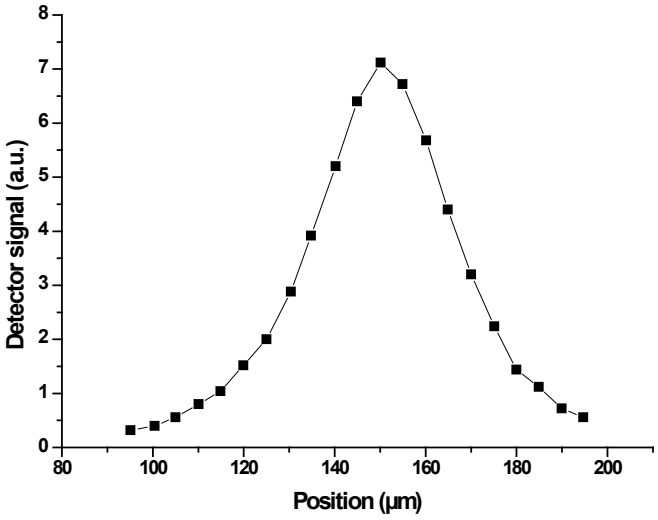

Fig. 9. Beam profile at the endtip's outer surface.

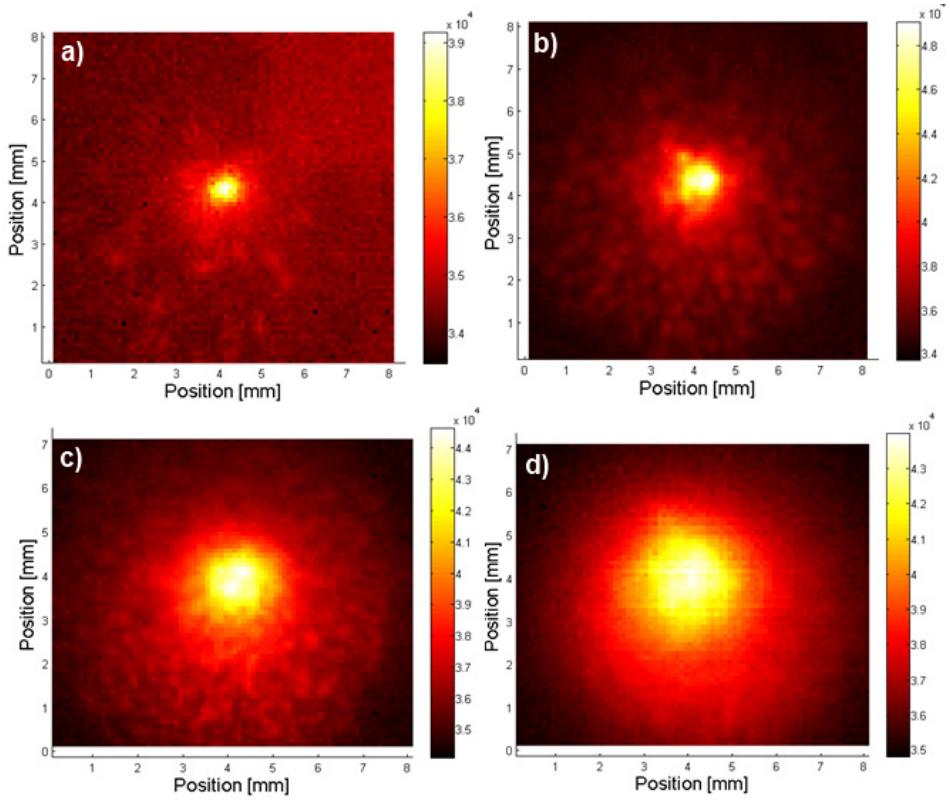

Fig. 10. Far-field profile of the fiber with endtip. Distance from the endtip to the reflective surface: (a) 10, (b) 20, (c) 50, and (d) 100 mm.

#176638 - $15.00 USD Received 20 Sep 2012; revised 14 Dec 2012; accepted 19 Dec 2012; published 21 Dec 2012

and the beam has more structure to it. These are most likely due the inside surface of the sapphire window not having an optical polish and the possibility of some contamination during construction of the endtip.

5. Tissue ablation

In order to demonstrate that the delivered power is sufficient to ablate hard and soft biological tissue, a sample of porcine tissue (bone and muscle) was used. The fiber length used for the ablation experiment was 2 m and the output end was sealed by the endtip shown in Fig. 8. The output power was 30 mJ which produced a fluence of >500 J/cm^2 at the output surface of the endtip. This energy density was sufficient to ablate the porcine muscle and bone as can be seen in Fig. 11. At these fluencies the ablation depth for a single shot on bone was approximately 200 µm and the heat-affected zone (HAZ) was about 70 µm (see Fig. 11(b). By adapting the laser parameter, the HAZ can be minimized, however the investigation of these parameters was not the scope of these experiments. In these trials the fiber was hand held, as opposed to being fixed, to simulate how it may be used in practice. A side effect of this is that the pulses are not delivered perfectly normal to the tissue. The fiber was used in contact mode and at different distances and also ablation was carried out in aqueous conditions with the fiber and tissue completely immersed in water (Fig. 12). These results clearly show that the fiber is capable of delivering pulses of the necessary energy for tissue ablation and shows that the fiber and endtip configuration is robust and can be handled in a practical manner.

Autoclaving was performed on the fiber. The fiber was sealed on both ends using an arc-fusion splicer to fuse the ends by localized melting. The conditions in the autoclave were 121°C at 15 psi for 15 min. No degradation of the fiber could be determined after repeating

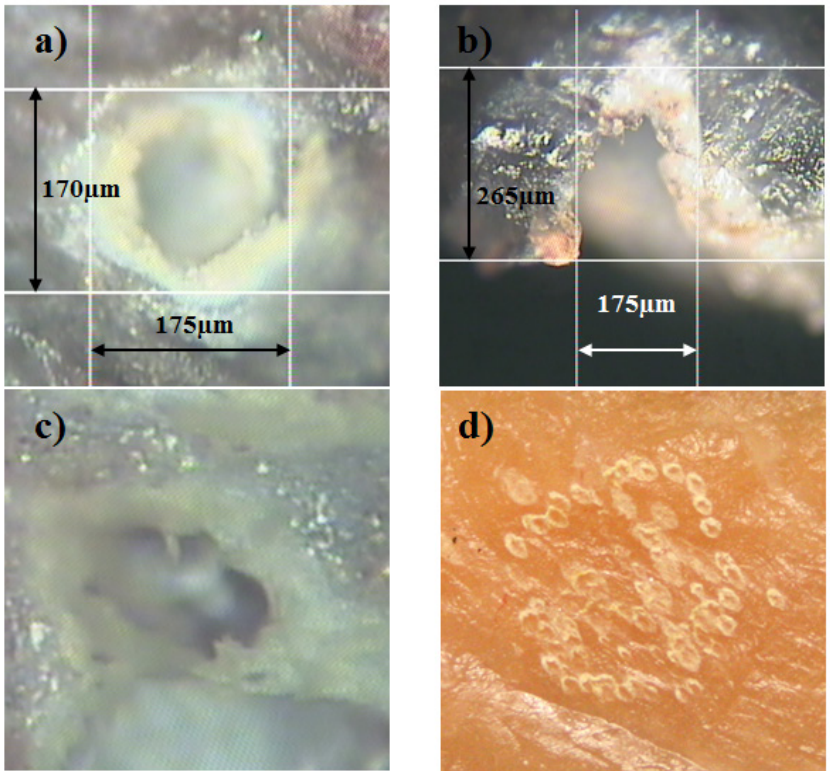

Fig. 11. Tissue ablation results: (a) porcine bone; (b) cross-section through hole in porcine bone showing ablation depth with single shot, ablation depth is 265 µm; (c) porcine muscle; (d) tissue ablation of porcine muscle with a number of shots being distributed over the surface.

#176638 - $15.00 USD Received 20 Sep 2012; revised 14 Dec 2012; accepted 19 Dec 2012; published 21 Dec 2012

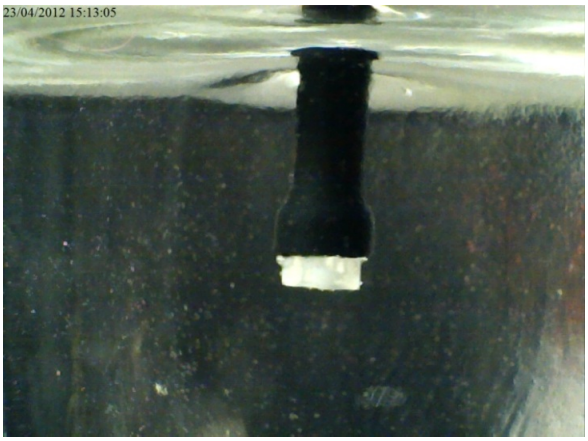

Fig. 12. Endtip immersed in water.

this procedure 3 times. At these temperatures a softening of the acrylic fiber jacket can be expected which could lead to localized weakening points. However for a medical device a polyimide jacket can be used, which withstands much higher temperatures. The endtip was not tested in the autoclave, however previous tests [15] have shown that the bond between the sapphire tube and sapphire rod is hermetically sealed and stable to temperatures over 1000°C.

To demonstrate the capabilities of the system of fiber and endtip the ablation of ovine bone is presented in Fig. 13(a) (Media 1). The width of the cut is around 300 µm with a depth of 220 µm. The square is 2x2 mm in size and the distance between tissue and endtip is around 5 mm. Additionally the ablation under water is shown in Fig. 13(b) (Media 2). As can be seen the tip is fully submerged into the water. Parameters in both experiments were kept the same.

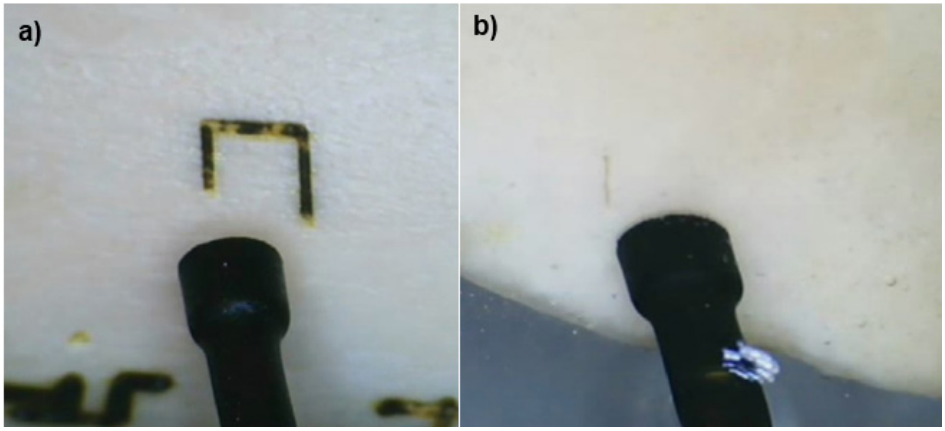

Fig. 13. Screenshots from Media 1 and Media 2. (a) Ablation of ovine bone in air. Square dimensions are 2x2 mm (Media 1) (b) Ablation of ovine bone under water (Media 2).

6. Conclusion

A novel delivery system for Er:YAG laser radiation is presented which has the potential to enable new minimally invasive surgical procedures. The flexible fiber is fabricated from silica and guides the light inside a hollow core by the ARROW principle which increases the damage threshold significantly, compared to a solid core fiber, and allows the effect of the high absorption of silica at this wavelength to be negated. The output beam profile is single-mode-like, leading to a significant advantage, in terms of controllability and stability for the delivered energy, compared to other large core fibers. The performance in terms of delivered fluence (up to 2300 J/cm^2) far exceeds the thresholds needed for biological tissue. This has

#176638 - $15.00 USD Received 20 Sep 2012; revised 14 Dec 2012; accepted 19 Dec 2012; published 21 Dec 2012

been practically demonstrated by showing that hard and soft tissue could be ablated. A practical approach for encapsulation of the fiber has been proposed which demonstrates that a practical surgical device could be developed. This system shows a promising alternative to the existing delivery systems already used in medicine and other high power applications at 2.94 μm and paves the way for novel minimally invasive surgical procedures.

Acknowledgments

This work was funded by the UK Engineering and Physical Sciences Research Council under grants EP/G039097/1 and EP/I011315/1. Thanks to Daniele Faccio for taking the photographs of the endtip (Fig. 8) and to M Squared Laser Ltd. for the loan of a Firefly-IR laser system.

#176638 - $15.00 USD Received 20 Sep 2012; revised 14 Dec 2012; accepted 19 Dec 2012; published 21 Dec 2012